Energy Conversion and Management: X 12 (2021) 100121

Contents lists available at ScienceDirect

Energy Conversion and Management: X

journal homepage: www.sciencedirect.com/journal/energy-conversion-and-management-x

Analysis and optimization of a modified Kalina cycle system for low-grade heat utilization

Mohammad Masrur Hossain [a,b], Niyaz Afnan Ahmed [b], Md Abid Shahriyar [b], M. Monjurul Ehsan [b], Fahid Riaz [c,d], Sayedus Salehin [b], Chaudhary Awais Salman [e,*]

[a] Department of Mechanical Engineering, University of Washington, 1959 NE Pacific St, Seattle, WA 98195, USA
[b] Department of Mechanical and Production Engineering, Islamic University of Technology, Board Bazar, Gazipur 1704, Bangladesh
[c] Department of Mechanical Engineering, National University of Singapore, 117575 Singapore, Singapore
[d] Mechanical Engineering Department, Abu Dhabi University, Abu Dhabi 59911, United Arab Emirates
[e] School of Business, Society and Engineering, Mälardalen University, SE 721 23 Västerås, Sweden

ARTICLE INFO

Keywords:
Kalina cycle system
Low-grade thermal source
Multi-phase expander
Thermodynamic analysis

ABSTRACT

Kalina cycle system (KCS) offers an attractive prospect to produce power by utilizing low-grade heat sources where traditional power cycles cannot be implemented. Intending to explore the potential of exploiting low-grade heat sources for conversion to electrical energy, this study proposes two modified power generation cycles based on KCS-34. A multi-phase expander is positioned between the Kalina separator and the second heat regenerator in the proposed X-modification. In contrast, it is located between the mixer and second regenerator for Y-modification. To explore the potential benefits and limitations of the proposed modifications contrasted with the KCS-34, thermodynamic modeling and optimization have been conducted. The influence of critical decision parameters on overall cycle performance is analyzed. The result elucidates that by implementing an additional multi-phase expander, a significant amount of energy can be extracted from a lean ammonia water loop and X-modification can deliver superior thermodynamic performance compared with the Y-modification and the original KCS-34. With a reduced turbine inlet pressure of 58 bar and an ammonia concentration of 80%, the X-modified cycle's efficiency reaches a peak value of 17% and a net power yield of 1015 kW. An increase of 6.35% can be achieved compared with the conventional KCS-34 operating at the same conditions. Maximum exergy destruction of the working substance was observed in the condenser.

Introduction

To sustain social and economic development, the energy shortage issue has to be appropriately addressed and one approach to resolve this critical issue is to utilize low-grade heat sources [1,2]. There are numerous sources of low-quality energy available, including industrial waste heat, geothermal energy, and solar thermal energy. However, due to their low grade, these heat sources cannot be efficiently used to generate electrical power using conventional methods [3,4]. As a result, modifications to the traditional power cycle system are required for low-grade energy conversion applications.

The ORC is a modified Rankine cycle that utilizes organic low boiling fluids as working fluids. This cycle has the potential to generate electricity from low-quality heat sources [5–8]. The recent performance analysis indicates that the condensation temperature, evaporation temperature, and evaporation pressure of the working fluid significantly influence the ORC cycle's performance [9,10]. However, due to the constant evaporation temperature, significant irreversibility is observed in the ORC cycle during the evaporation process [11].

Several antiquated fossil-fuel-fired steam power plants are still operational in countries with large fossil-fuel reserves exhibiting quite a minimal efficiency [12,13]. Nearly 29% of net effective efficiency is obtained for the entire fleet of conventional power plants, although a higher net effective efficiency of 33% can be achieved when 500 MW units function together [14,15]. According to estimation, at least 1–2 percentage additional efficiency can be further achieved for existing power plants [16]. To increase the efficiency of the power generation units while minimizing environmental degradation, a viable source is the low-grade heat generated by these power plants' exhaust, which can be converted to electricity. However, these low-grade exhaust gases lack the thermal energy necessary to generate steam.

* Corresponding author.
E-mail addresses: fahid.riaz@u.nus.edu (F. Riaz), awais.salman@mdh.se (C. Awais Salman).

https://doi.org/10.1016/j.ecmx.2021.100121
Received 29 May 2021; Received in revised form 27 September 2021; Accepted 18 October 2021
Available online 23 October 2021

Nomenclatures

T	Temperature (K)
P	Pressure (bar)
E	Exergy (kJ)
S	Entropy (kJ/K)
m	Mass flow rate (kg/s)
h	Specific enthalpy (kJ/kg)
I	Thermal irreversibility (kJ)
Q	heat transfer rate (kW)
W	Power (kW)
x	Ammonia concentration
X	Vapor quality
c	Specific heat (kJ/kg-k)

Greek Letter

η	Efficiency (%)

Subscripts

0	Ambient Condition
1–14	System's State
in	Heat input
out	Heat output
rm	Rich mixture
lm	Lean mixture
KS	Kalina separator
boi	Boiler
cond	Condenser
Regen	Regenerator
thr	Throttle valve
sep	Separator
c	Cooling water
p	Pump
Tur, A	Turbine A
EX	Multi-Phase Expander
ex	Exergy
KCS	Kalina cycle system
ORC	Organic Rankine cycle
TFC	Trilateral Flash cycle
gen	Generator
cw	Cooling water

In an effort to improve the efficiency of thermodynamic cycles, Dr. Kalina proposed a new genre of power generation cycle in the 1980 s, named the Kalina cycle, that utilized an ammonia-water mixture as the working substance [17]. This power generation cycle was designed to utilize medium to low-grade heat source applications [18]. The Kalina cycle is widely regarded as the most significant advancement in thermal power cycle design since the invention of the Rankine cycle in the mid-1800s [11]. Kalina cycle is considered to be one of the few competitors of the ORC [17]. Depending upon the heat sources' temperature, the Kalina cycle system is categorized as KCS-5 to utilize waste heat from a direct-fired power plant, KCS-6 to integrate with a gas turbine-based combined cycle power plant, KCS-11 to utilize geothermal energy ranging between 121 °C to 204 °C, KCS-34 to utilize heat sources below 121 °C [17,19]. The Kalina cycle indicates a decrease in the irreversibility of the evaporation process when compared to the ORC cycle operating under similar input conditions [20]. Among the different categories of the Kalina cycle, the KCS-11 and KCS-34 configurations are well-known for their effectiveness in utilizing low-grade heat sources.

A KCS 34-based power plant was constructed at the Hoechst industrial park, using the combined heat and power plant's dry flue gas as the input source. This project considerably increases the cooling process's efficiency and presents a viable waste-heat-to-electricity conversion technology [21]. The maximum power output and efficiency of the KCS-34 were observed at 78% ammonia concentration in working fluid for Indonesian environmental conditions and for Icelandic environmental conditions, this value of ammonia mass fraction is 82% [11]. The KCS-11 operating at moderate pressure has exhibited better output when compared with the ORC cycle [22]. The Kalina cycle for the combined cooling and power application has gained significant attention in recent years [23,24]. The Kalina cycle for the combined power generation and cooling application proposed by Vidal et al. has an exergy efficiency of 37.3 % and an overall thermal efficiency of 24.2 % [25]. A novel ammonia-water-based cycle for the combined cooling and power application proposed by Liu and Zhang [26] indicates an effective reduction in energy consumption compared to the traditional cycle. Research on solar integrated Kalina system with auxiliary superheater has demonstrated higher feasibility and efficiency than the conventional solar power generation system [27]. Nan et al. conducted a life cycle assessment and optimization of a Kalina cycle integrated absorption chiller and observed better environmental performance of this proposed system compared with the individual Kalina cycle [28]. The possibility of integrating green compressed air energy storage with the Kalina cycle was analyzed by Soltani et al. [29]. Two novel combined cooling, heating and power based on the Kalina cycle were presented by Rostamzadeh et al. [30]. Their analysis observed the Kalina-based CCHP cycle's superiority in terms of efficiency and economic performance compared with the ORC-based CCHP cycle. Modified Kalina cycle driven by the waste heat recovered from the Gas Turbine-Module Helium Reactor system was proposed by Parikhani et al. [31]. 4E analysis and optimization of the triple Gas Turbine-Rankine cycle-Kalina cycle were presented by Ozkan et al. They concluded that this system could recover 46.39% of total heat [32]. A novel solar-driven triple effect absorption refrigeration system integrated with the Kalina cycle was proposed by Gogoi et al. [33]. A thermoelectric generator (TEG) integrated Kalina cycle-based CCHP system was analyzed by Malik et al., considering low-grade geothermal sources as the energy source. They concluded the integration of TEG with the base system can improve the efficiency by 1.7% [34]. Congcong et al. [35] followed a novel pinch-based mathematical approach to optimize the Kalina cycle. Mohammadkhani et al. designed a zero-dimensional model to simulate the Kalina cycle for high-temperature applications [36]. Transcritical CO2 integrated KCS-11 was analyzed from the exergoeconomic point of view by Abdolalipouradl et al. They observed a thermal efficiency of 16.63% and exergy efficiency of 63.78% [37]. Mojtaba et al. presented a new designing and optimizing method of Kalina cycle power plant driven by the linear parabolic solar collector and concluded that it could reduce operating time and system cost when the proposed improvement was implemented [38]. Triple pressure Kalina cycle combined with a refrigeration cycle for cogeneration applications was proposed and examined by Zhang et al. [39]. A novel power production framework has been introduced by Hayder et al., which incorporates the Kalina cycle and the retention refrigeration cycle [40].

To extract energy from the lean ammonia-water mixture, the two-phase expander plays a critical role. In recent years, a significant amount of research has been conducted to increase the two-phase expander's efficiency [41]. An efficiency of 75% has been exceeded when the two-phase expander is integrated on TFC (Trilateral Flash cycle) [42]. The two-phase expander technology used in the waste heat energy recovery system is feasible, and the cost rate is not that substantial [43–46].

The research conducted on the Kalina cycle either focuses on parametric analysis or tries to introduce a novel Kalina cycle. However, the

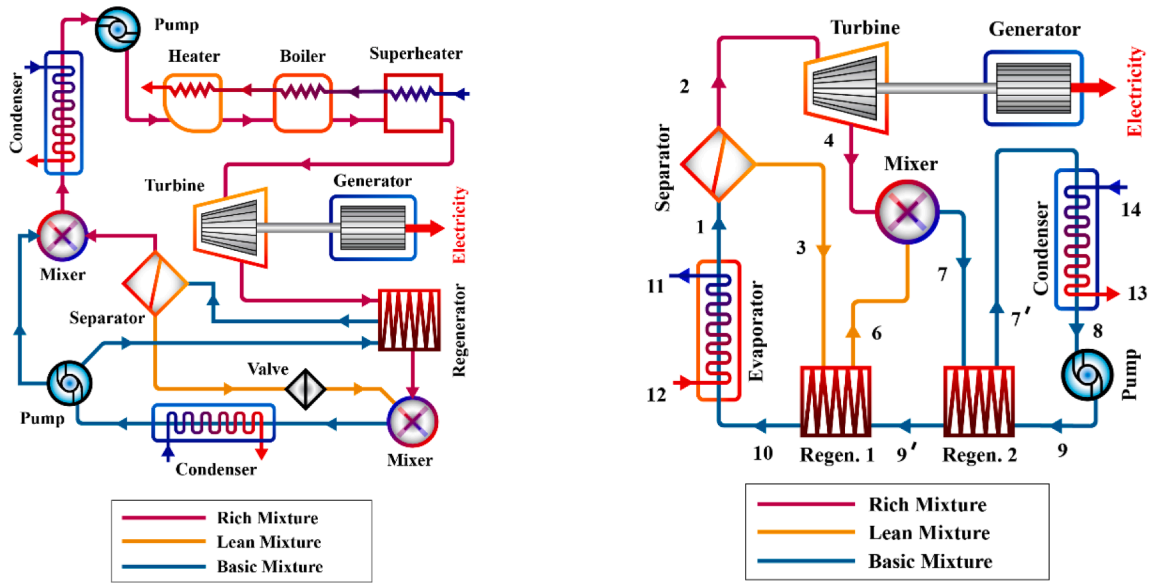

Kalina cycle Proposed by Dr. Kalina

KCS-34

Fig. 1. Schematic Diagram of Kalina cycle System

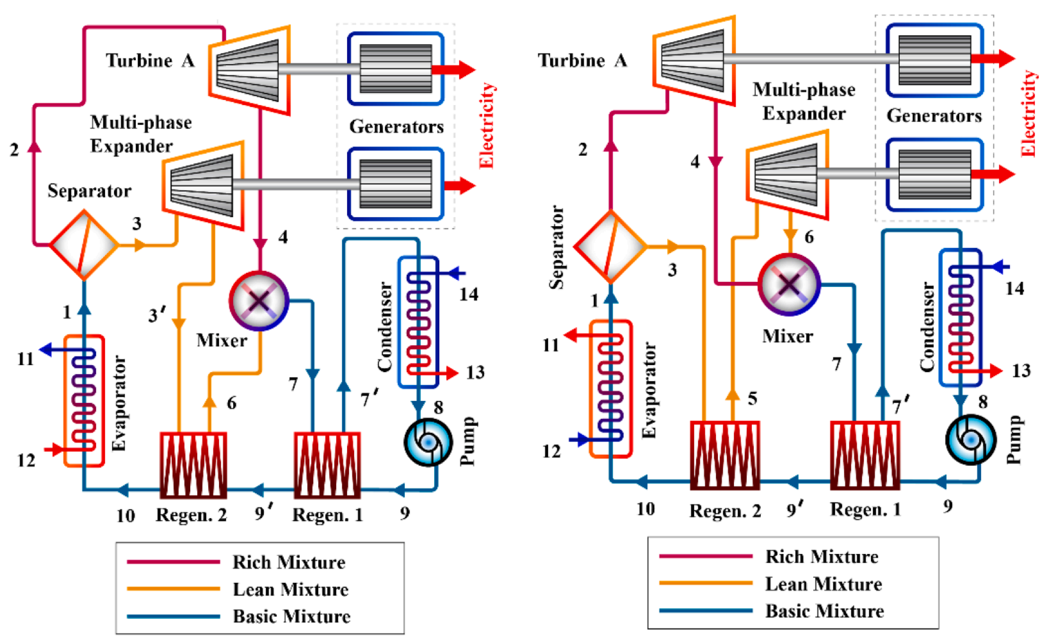

X-modified cycle

Y-modified cycle

Fig. 2. The modified Kalina cycle system.

lean ammonia-water mixture in the close loop of the KCS-34 is hardly analyzed, although it contains significant enthalpy, from which substantial energy can be extracted. Two novel KCS systems have been developed in the present work, integrating an additional two-phase expander in the lean ammonia-water loop of the KCS-34. Additionally, to the authors' knowledge, no research articles containing a detailed methodology for optimizing KCS-34 have been published to date; thus, this research presents a comprehensive model for solving and optimizing KCS-34. Since KCS-34 is designed to generate electricity through the conversion of low-grade heat; it is well suited to extracting energy from industrial flue gases.

The thermal performance of the proposed Kalina cycle is compared to that of the KCS-34. To simulate the Kalina cycle System under steady-state conditions, a mathematical model has been developed. To examine the influence of critical decision parameters on system performance, a parametric analysis has been conducted. Furthermore, pressure

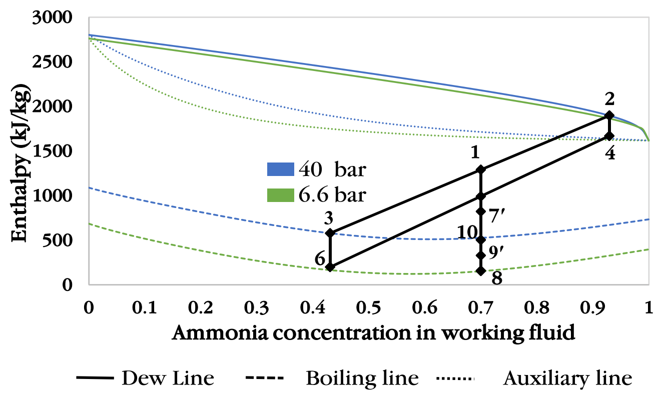

Fig. 3. h-x diagram of Kalina cycle System. The Blue lines indicate working fluid properties at 40 bar and the green lines indicate working fluid properties at 6.6 bar. (For interpretation of the references to colour in this figure legend, the reader is referred to the web version of this article.)

optimization of the working fluid has also been performed.

System description

Fig. 1 represents the original Kalina cycle introduced by Kalina in which an additional condenser operating at an intermediate pressure was placed after the binary separator providing an extra degree of freedom in the boiling mixture's composition, which subsequently allowed the distillation process at a lower pressure than the Kalina cycle's maximum pressure [18]. Another difference compared to KCS 34 is in the heat exchanger's position, which had to be installed downstream of the expander [17].

In the circumstances when low or medium graded heat sources are used and the power conversation unit is smaller, the power cycle layout is simplified, consisting of only one main condenser working at the cycle's lowest temperature and placing the evaporator before the separator [47]. Several researchers have investigated this simplified Kalina cycle to derive the best possible combination of the working fluid characteristics and the operating conditions [48,49].

In Fig. 1, the schematic diagram of KCS-34 is also presented. When heat from the source is directed to the Kalina evaporator (11,12), saturated ammonia-water mixture absorbs energy (1,2) and gets superheated. In the separator, lean ammonia-water mixture (2,3) gets separated from the rich ammonia-water mixture (2,4). By expanding the superheated rich ammonia-water mixture, work is produced by the expander (2,4). After leaving the turbine, this exhaust-rich ammonia-water mixture is diluted with the lean ammonia-water mixture in the mixing chamber (4,6,7). Following the mixing procedure, condensation of the working fluid proceeds (7',8). After that, using a pump, the saturated working fluid's pressure is raised (8,9) to an intermediate pressure then heated in the pre-heater (9,9',10). Two regenerative heat exchangers are used as a medium to pre-heat the working substance utilizing the internal residual heat of the cycle [50]. This working procedure is also illustrated in the h-x diagram in Fig. 3.

An explanation of the efficiency improvements for the KCS cycle can be derived by explaining the heat acquisition and the heat rejection process. Due to the ammonia-water mixture's unique condensing and boiling properties, the exergy losses in the heat exchanger and the thermal pinch effect in the boiler gets decreased, resulting in a better efficiency performance.

Depicted in Fig. 2, the proposed two modifications of KCS-34, termed the X-modified cycle and the Y-modified cycle, are introduced to define the most efficient arrangement of the multi-phase expander. Coupled with KCS-34, all three cases of KCS-34 have been investigated comprehensively. The investigated cases are described as:

i. X-modified cycle: In the conventional KCS-34, lean ammonia-water mixture separated from the working fluid is passed through the lean ammonia-water loop. During this process, a small fraction of lean ammonia-water's available energy gets extracted at the regenerator. However, if an expander is installed in the lean ammonia-water loop, it can recover a significant portion of available energy. So, with the purpose of extracting additional energy from the lean ammonia loop of KCS 34, a modification of KCS 34 is presented in Fig. 2. In the KCS-34 layout, a multi-phase expander in addition to the vapor expander is proposed to be positioned intermediate of the regenerator and the separator to derive the X-modified cycle.
ii. Y-modified cycle: With the purpose to find out the most efficient layout of modified KCS-34, another modification is present in Fig. 2, termed as Y-modification. In this modification, the multi-phase expander is placed intermediate of the regenerator and the mixer.
iii. KCS-34: With a view to comparing KCS-34 with the proposed cycles, KCS 34 presented in Fig. 1 is also investigated.

Methodology

Assumptions

i. All three cycles are considered to be operating at the steady-state condition.
ii. Pressure drops and heat losses are neglected in this system, including the pipes and heat exchangers.
iii. The process of pumping is assumed to be isentropic.
iv. The dry saturated vapor is approximated at the turbine inlet (state 2).
v. The mixing process in the mixing chamber is isentropic.
vi. The Log Mean Temperature Difference (LMTD) values of condenser, Kalina evaporator, and regenerators are held constant throughout the parameters' sensitivity analysis for each different cycle.
vii. At the condenser outlet, working fluid is assumed to be saturated (state 8).
viii. The inlet temperature of cooling water constrains working fluids temperature at the condenser exit (state 8) such that no temperature cross-over occurs.
ix. The isentropic and mechanical efficiencies of the multi-phase expander in X-modification and Y-modification are identical.
x. In X-modification and Y-modification, the effectiveness of the regenerator is identical to its counterpart in KCS 34.

Mathematical model

To obtain a comprehensive understanding of the function of the multi-phase expander, qualitative exergy and quantitative energy investigations are carried out. For example, in the case of the X-modified cycle, the multi-phase expander's work yield can be denoted as:

$$W = m \times (h_3 - h_3') \quad (1)$$

The h-x diagram depicted in Fig. 3 graphically illustrates the mathematical formulation of KCS-34. The measures of the lines in the perpendicular orientation designate the quantity of qualitative energy transferred to the system. Considerable thermal energy is interchanged in the recuperator of the saturated lean ammonia-water mixture, geometrically indicated by line 3–6.

The quantitative thermodynamic analysis can be presented for these cycles by establishing the Energy balance relationships among each component. The heat input of the system (Q_{in}):

$$Q_{in} = m_h(h_{12} - h_{11}) \quad (2)$$

The exhaust gas from a combined power cycle's topping cycle is used

Table 1
Boundary conditions for the Kalina Cycle's under investigation [50,52].

Input parameters	Status quo
Flue gas flow rate	112 kg/s
Flue gas temperature at the evaporator inlet	150 °C
Flue gas temperature at the evaporator outlet	130 °C
Flue Gas composition	
Oxygen	5.0 % volume
Nitrogen	75.2 % volume
Argon	0.9 %volume
H_2O	5.6 % volume
SO_2	0.04 % volume
CO_2	13.3 % volume
Condensation pressure	6.6 bar
Generator efficiency	96%
Turbine isentropic efficiency	87%
Pump isentropic efficiency	80%
Mechanical efficiency	98%
The cooling water inlet temperature	5 °C
Minimum temperature differences	
Evaporator	6 K
Regenerator	4 k
Condenser	3 K

as the heat source in this research, and the amount of energy exchanged in the evaporator is equal to the system's heat input. The system's heat source is consistent since the temperature of the flow from the heat reservoir is fixed at the inlet.

Quantification of thermal energy exchanged during condensation in the condenser (Q_{cond}):

$$Q_{cond} = m \times \left(h_7^{'} - h_8\right) \tag{3}$$

Heat transfer in the regenerators (regen.1 and regen.2):

$$Q_{regen.1} = m \times \left(h_9^{'} - h_9\right) \tag{4}$$

$$Q_{regen.2} = m \times \left(h_{10} - h_9^{'}\right) \tag{5}$$

The amount of power generated by the Turbine, A ($W_{Tur,A}$) was determined by multiplying the mass flow rate of the rich ammonia-water mixture (m_{rm}) with the enthalpy drop:

$$W_{Tur,A} = m_{rm} \times (h_2 - h_4) \tag{6}$$

Similar to the turbine, Expander's power yield (W_{EX}) was calculated by multiplying the mass flow rate of the lean ammonia-water mixture (m_{lm}) with the enthalpy drop:

For X modified cycle,

$$W_{EX} = m_{lm} \times \left(h_3 - h_3^{'}\right) \tag{7}$$

For Y modified cycle,

$$W_{EX} = m_{lm} \times (h_5 - h_6) \tag{8}$$

$$W_p = m \times (h_9 - h_8) \tag{9}$$

$$W = W_{Tur,A} + W_{EX} - W_p \tag{10}$$

Exergy analysis can be applied to determine the potential work lost due to irreversibility at a specific dead state [19]. Assuming the environmental pressure and temperature are P_o, T_o. The exergy destruction in each component of KCS 34 and modified cycles are calculated.

The exergy loss in the Kalina evaporator (I_{KE}):

$$I_{KE} = T_o \times \left\{m \times (s_1 - s_{10}) - \frac{Q_{in}}{T_{mean}}\right\} \tag{11}$$

The exergy loss in the Kalina separator (I_{KS}):

$$I_{KS} = T_o \times \{m_{rm} \times (s_2 - s_1) + m_{lm} \times (s_3 - s_1)\} \tag{12}$$

For X modification,

The exergy loss in both regenerators:

$$I_{regen.2} = T_o \times \{m_{lm} \times (s_6 - s_3') + m \times (s_{10} - s_9')\} \tag{13}$$

$$I_{regen.1} = T_o \times \{m \times (s_7' - s_7) + m \times (s_9' - s_9)\} \tag{14}$$

The exergy loss in the turbine:

$$I_{Tur,A} = T_o \times m_{rm} \times (s_4 - s_2) \tag{15}$$

The exergy loss in the multi-phase expander (I_{EX}):

$$I_{EX} = T_o \times m_{lm} \times \left(s_3^{'} - s_3\right) \tag{16}$$

The exergy loss in the absorber ($I_{absorber}$):

$$I_{absorber} = T_o \times \{m_{rm} \times (s_7 - s_4) + m_{lm} \times (s_7 - s_6)\} \tag{17}$$

For Y modification,

The exergy loss in both regenerators:

$$I_{regen.2} = T_o \times \{m_{lm} \times (s_5 - s_3) + m \times (s_{10} - s_9')\} \tag{18}$$

$$I_{regen.1} = T_o \times \{m \times (s_7' - s_7) + m \times (s_9' - s_9)\} \tag{19}$$

The exergy loss in the turbine, A ($I_{Tur,A}$):

$$I_{Tur,A} = T_o \times m_{rm} \times (s_4 - s_2) \tag{20}$$

The exergy loss in the multi-phase expander (I_{EX}):

$$I_{EX} = T_o \times m_{lm} \times (s_6 - s_5) \tag{21}$$

The exergy loss in the absorber ($I_{absorber}$):

$$I_{absorber} = T_o \times \{m_{rm} \times (s_7 - s_4) + m_{lm} \times (s_7 - s_6)\} \tag{22}$$

The exergy loss in the condenser (I_{cond}):

$$I_{cond} = m \times \{(h_{7_1} - h_8) + T_o \times (s_{7_1} - s_8)\} \tag{23}$$

The exergy loss in the pump (I_p):

$$I_p = T_o \times m \times (s_9 - s_8) \tag{24}$$

The total amount of exergy lost:

$$I = I_{KE} + I_{KS} + I_{regen.1} + I_{regen.2} + I_{Tur,A} + I_{EX} + I_{cond} + I_p + I_{absorber} \tag{25}$$

The second law of efficiency is defined by the ratio of exergy yield to exergy input. The degree of irreversibility limits the exergy yield of the cycle [51].

The exergy efficiency (η_{ex}):

$$\eta_{ex} = \frac{W}{E_{in}} \tag{26}$$

E_{in} and E_{out} are the exergy values at the heat source's inlet and outlet, respectively.

$$E_{in} = m_h \times c_h \times [T_{11} - T_o - T_o - \ln(\frac{T_{11}}{T_o}) \tag{27}$$

$$E_{out} = m_h \times c_h \times [T_{12} - T_o - T_o - \ln(\frac{T_{12}}{T_o}) \tag{28}$$

The LMTD of three distinct categories of heat exchangers is calculated. For example, the LMTD functions for the Y-modified cycle can be expressed as

$$\Delta T_{\text{Kalina evaporator}} = \frac{[(T_{12} - T_{10}) - (T_{11} - T_1)]}{\ln\left(\frac{T_{12} - T_{10}}{T_{11} - T_1}\right)} \tag{29}$$

$$\Delta T_{\text{cond}} = \frac{[(T_7' - T_{14}) - (T_8 - T_{13})]}{\ln\left(\frac{T_7' - T_{14}}{T_8 - T_{13}}\right)} \tag{30}$$

Table 2
Model Validation with literature.

Component	Parameter	KCS-34 (Husavic Power Plant)	KCS-34 (simulated using EBSILON®Professional)	Deviation (%)
Pump	P_9	35.3 bar	35.3 bar	0 %
	T_9	8 °C	8.214 °C	2.6 %
	Power consumption	96.1 kW	96.623 kW	0.5 %
Regenerator 1	P_{10}	33.3 bar	33.3 bar	0 %
	T_{10}	63 °C	63.118 °C	0.2 %
Regenerator 2	P_9'	34.3 bar	34.3 bar	0 %
	T_9'	41 °C	40.456 °C	1.3 %
Evaporator	P_1	32.3 bar	32.3 bar	0 %
	T_1	116 °C	116 °C	0 %
	T_{11}	80 °C	80 °C	0 %
	T_{12}	122 °C	122 °C	0 %
Turbine	T_2	116 °C	116 °C	0 %
	T_4	43 °C	42.734 °C	0.6 %
	P_4	6.6 bar	6.6 bar	0 %
Condenser (Cooling water)	$T_{7\text{-}1}$	30 °C	29.821 °C	0.6 %
	T_8	8 °C	7.537 °C	6 %
Generator	Gross electric power	2194.8 kW	2208.339 kW	0.6%

$$\Delta T_{\text{regen.1}} = \frac{[(T_7 - T_9') - (T_7' - T_9)]}{\ln\left(\frac{T_7 - T_9'}{T_7' - T_9}\right)} \tag{31}$$

$$\Delta T_{\text{regen. 2}} \frac{[(T_3 - T_{10}) - (T_5 - T_9')]}{ln\left(\frac{T_3 - T_{10}}{T_5 - T_9'}\right)} \tag{32}$$

Boundary condition

The EBSILON®Professional software package was used to determine the thermal properties of the working fluid and the thermodynamic performance of all the cycles. Initial conditions for the base model are presented in Table 1.

Optimization

Genetic algorithm (GA) provided by the EBSILON®Professional software package was used to optimize the Kalina cycles under investigation. Optimization was done following the stated steps:

I. Operating condition of the Kalina cycles such as ammonia mass fraction, pressure and temperature at the separator inlet, the pressure at the turbine and multi-phase expander outlet, the efficiencies of the generator, pump, turbine, the inlet and outlet temperature of the cooling water, the minimum pinch point temperature difference(PPTD) values of the condensers,

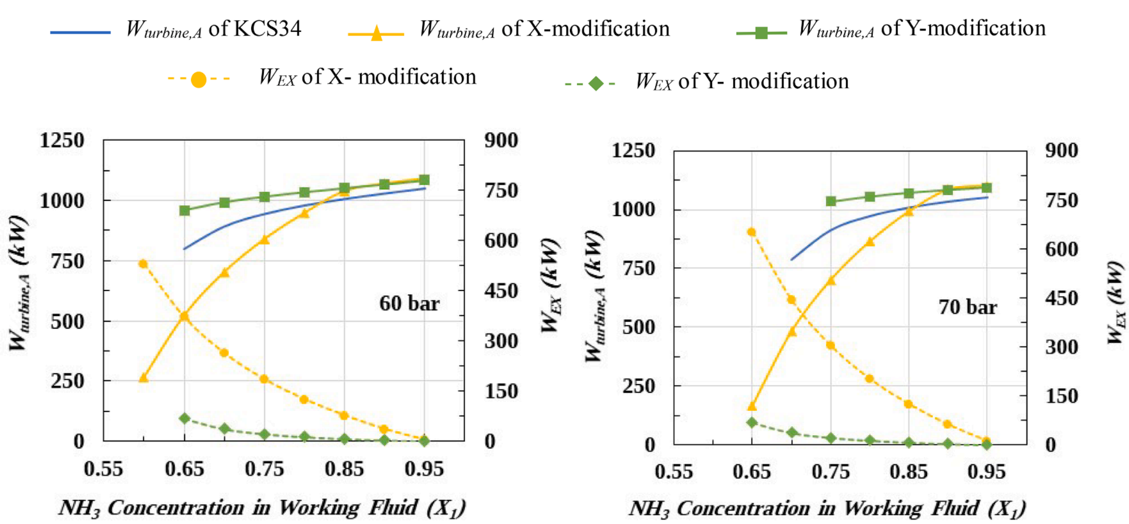

Fig. 4. The Power yield of turbine A and multi-phase expander with varying X_1 at various turbine inlet pressure.

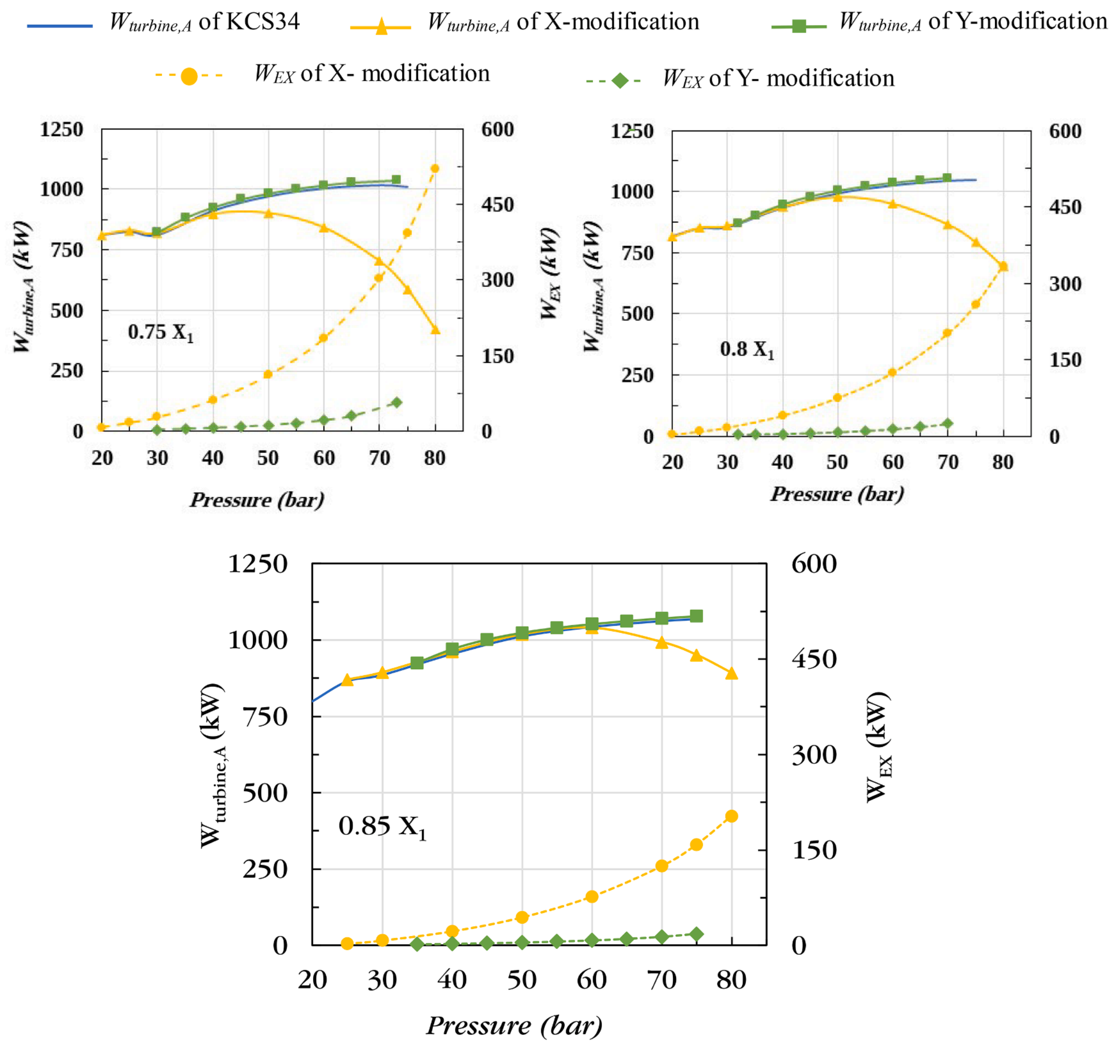

Fig. 5. The Power yield of turbine A and multi-phase expander with varying P_2 at various ammonia concentrations.

regenerators were given as the boundary parameters to the GA. Additionally, the GA was constrained by specifying the upper and lower limits of the boundary parameters.

II. Based on the initial population provided with the input parameters, GA does the optimization procedure covering the entire search region and with each iteration, it gradually moves towards the optimum solution.
III. The optimization process is segmented into two stages: During the first stage, the global maxima are located within the lower and upper limits. This stage makes sure that global maxima is achieved instead of local maxima.
IV. If an error occurs during the calculation of the thermodynamic properties or if an energy or mass balance could not be achieved with a residual equal to or less than 0.001 %, the solution is discarded.
V. In Diagram 1, a detailed optimization algorithm for the KCS-34 is presented as an example. Based on this, algorithms for the proposed Kalina cycles were developed.

Results and discussion

Model validation

At a steady-state operating condition, the simulation results have been validated against the real-world data of the KCS 34 cycle-based Husavic geothermal power plant in Iceland [50]. As it can be seen in Table 2, the results indicate a high degree of agreement between the simulation results and the data obtained from the Husavic power plant.

Sensitivity analysis on turbine performance

Apart from the pressure losses in pipes, heat regenerators, and absorber, there remain two critical pressure parameters in all the cases of KCS-34; the working fluid's pressure entering the turbine (P_2) and leaving the turbine (P_4). But P_4 is a dependent parameter as the cooling water's condition constrains it. Therefore, under a specific cooling condition and ammonia mass fraction in the working fluid, P_4 can't influence the performance of KCS-34. The ammonia concentration in the working fluid at the evaporator (X_1), the temperature of the working fluid leaving the Kalina separator (T_1), and entering the turbine (T_2) also influence the performance of the KCS-34 to a great extent. However, T_1 is approximately indistinguishable from T_2 as pressure and thermal losses were disregarded during the investigation of all modified KCS-34. Subsequently, X_1 and P_1 are the independent parameters in all the instances of KCS-34, and these parameters are considered to be the critical parameters.

Effect of ammonia mass fraction

At a fixed evaporation pressure and cooling condition, the Kalina cycle's working fluid containing high ammonia mass fraction tends to evaporate at a greater extent due to ammonia's low boiling point than water. As a result, in all cases of KCS 34, as the ammonia mass fraction of

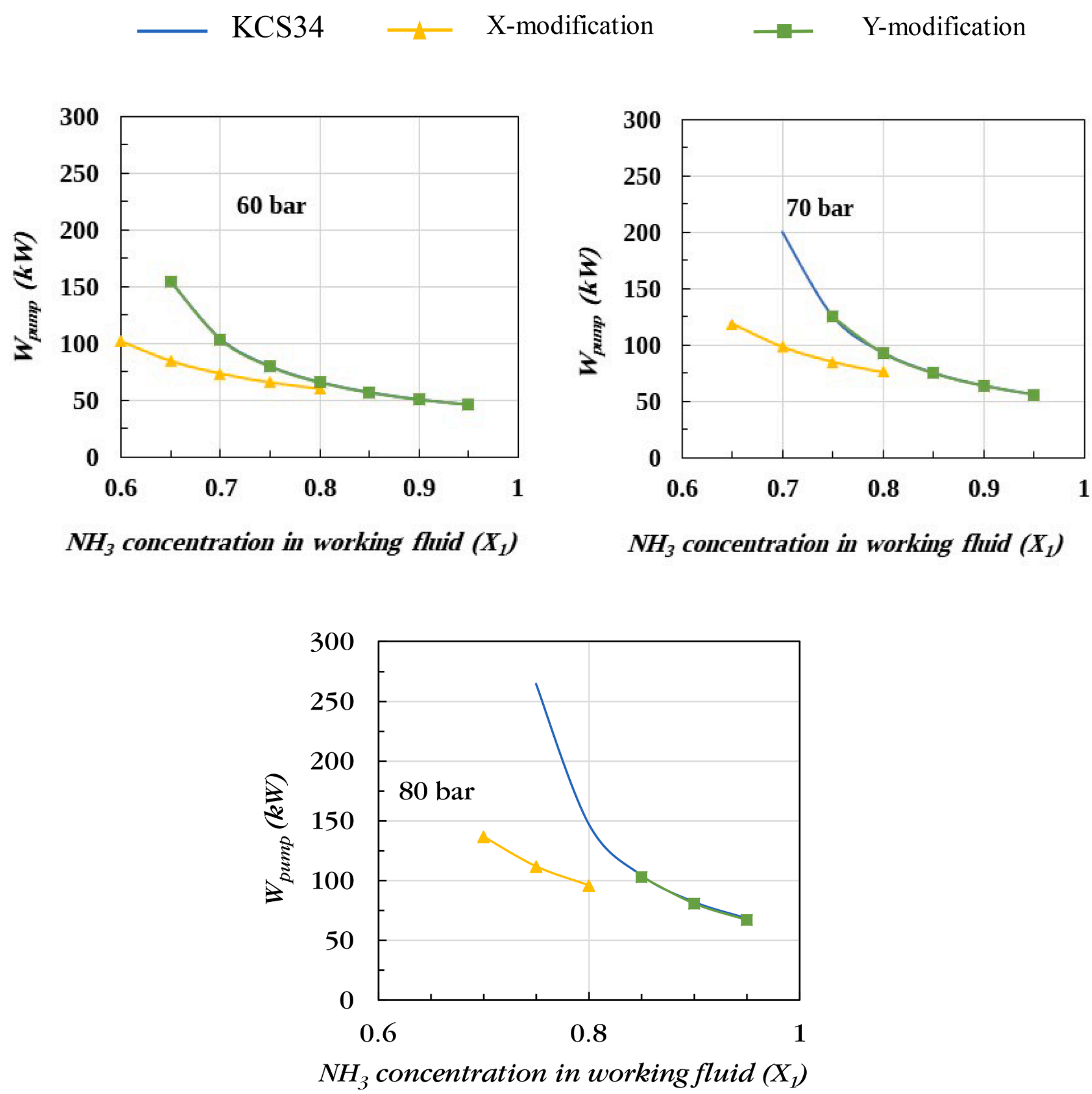

Fig. 6. Pump power consumption with varying X_1 at various turbine inlet pressure.

the working fluid increases, Turbine A's work output increases due to the increased mass flow of the rich ammonia-water mixture. This results in a decrease in the mass flow of the lean ammonia-water mixture through the multi-phase expander, resulting in decreased power output from the multi-phase expander.

Fig. 4 visually represents turbine A and multi-phase expander's power yield with the changing ammonia concentration on the working fluid for different turbine inlet pressures. As the heat source remained constant for all cases, therefore the work output of the multi-phase expander and the work output of the turbine both are expressed in the same group of graphs. Though both of the modifications were designed to extract energy from the lean ammonia water loop, their performance shows a particular distinction. In terms of turbine A's work output, KCS-34 performs better than the X-modification when the ammonia concentration is on the lower end; however, at a higher ammonia mass fraction, the type X modification surpasses the KCS-34. For example, at 80 bar and 0.7 ammonia concentration, the work output of KCS-34′s X modification is 38.4 percent less than that of KCS-34, but at 0.86 ammonia fraction, the work output of X modification exceeds that of KCS-34, and at 0.95 ammonia concentration, it exhibits a 4 percent higher work yield than KCS-34. However, in all cases, type Y modification shows a slightly higher turbine A output than the KCS-34, but with the decreasing P_2, this slight increment gets considerably slenderer.

Turbine B of the X-modified cycle provides the most impressive performance at high pressure and low concentration. As the concentration increases, the power yield from the multi-phase expander decreases; however, as the pressure increases, the power output from both of the proposed cycle's multi-phase expanders increases. However, the most significant rise is observed in the case of X-modification, and at a certain operating condition, multi-phase expander's work yield surpasses Turbine A. In contrast, for Y-modification, the multi-phase expander's performance is significantly less in comparison with Turbine A.

Effect of turbine inlet pressure

The boiling point of the ammonia-water mixture rises with the increasing pressure under a constant heat input condition, resulting in

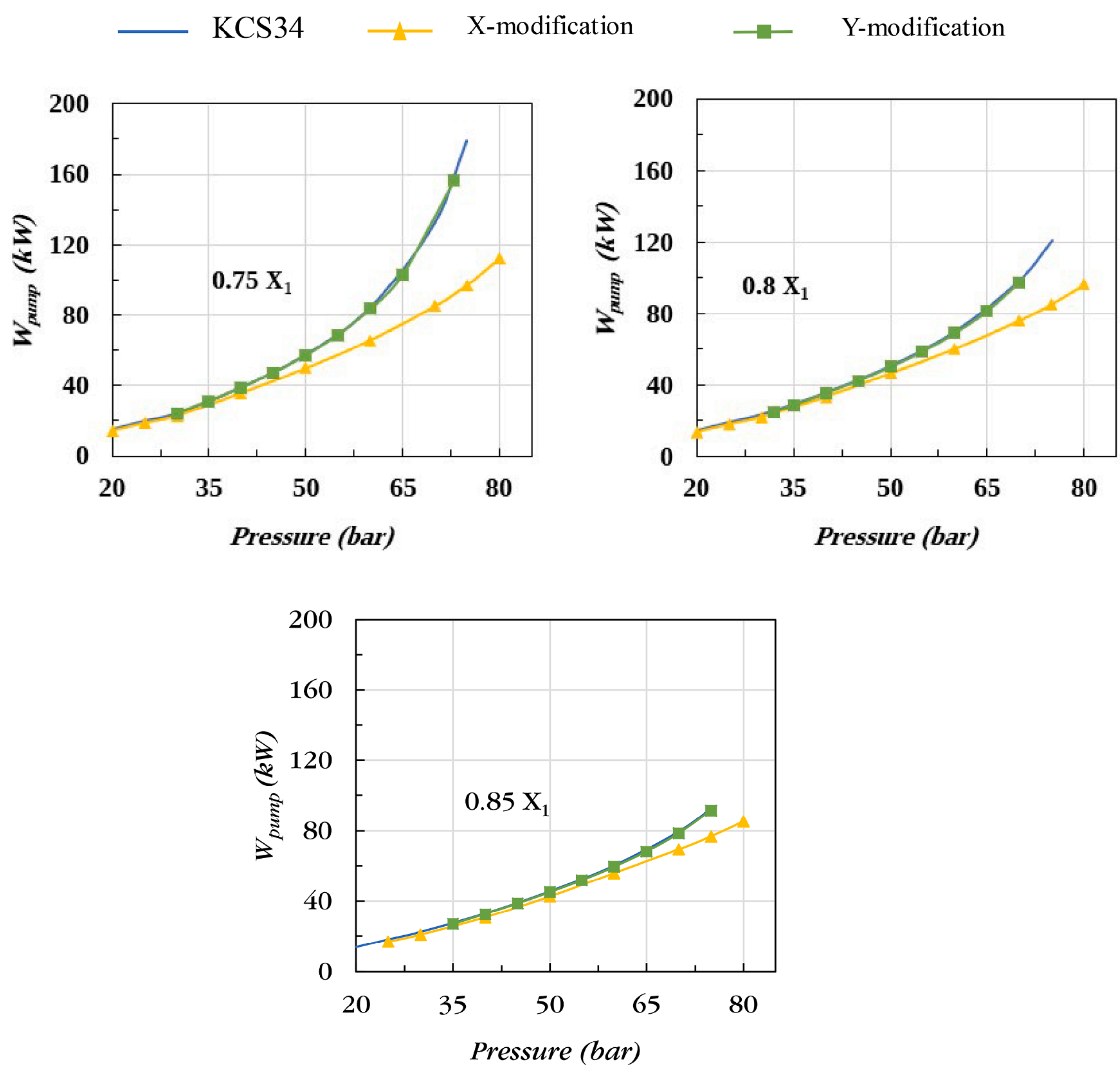

Fig. 7. Pump power consumption with varying P_2 at various ammonia concentrations.

an increment of the liquid phase in a two-phase flow condition. This boosts the mass flow in the lean ammonia-water loop, thereby enhancing the power output of the multi-phase expander. As the mass flow in the lean ammonia-water mixture loop rises, the mass flow in the rich ammonia-water mixture loop declines. However, for a constant cooling condition, the power output of the turbine increases proportionately to the increase in turbine inlet pressure. As a result of these simultaneous effects, turbine A's power output increases up to a certain value with the rising turbine inlet pressure and after that certain pressure value, Turbine A's power yield decreases significantly due to a significant decrease in the mass flow rate of the working fluid.

Fig. 5 illustrates the work output of turbine A and the multi-phase expander as the turbine inlet pressure changes for a given ammonia mass fraction in the working fluid. With increasing turbine inlet pressure, a nearly linear increase in power output is observed for the Y modification and KCS-34. In comparison, the type X modification turbine A exhibits a peak. A higher turbine inlet pressure is required to achieve this peak power output condition as the ammonia mass fraction increases. The work yield of the multi-phase expander increases with increasing turbine inlet pressure in all modifications of the KCS-34. However, type X modification is highly susceptible to the turbine's inlet condition; in comparison, type Y modification exhibits only a slight variation.

Sensitivity analysis on pump performance

Effect of ammonia mass fraction

As the concentration of ammonia in the working fluid increases, the specific volume of the working fluid decreases, resulting in reduced power demand to raise the working fluid's pressure by a specified amount. The correlation between pump power consumption and ammonia mass fraction in the working fluid is illustrated in Fig. 6. The pump power consumption for all KCS-34 modifications decreases as the ammonia concentration increases at constant pressure and mass flow rate. Moreover, with the decreasing P_2, the power consumption of the pump decreases. At similar operating conditions, both proposed cycles consume less energy than the conventional KCS-34 cycle. However, a marginal reduction in pump power consumption is observed when the Y-modification is implemented, whereas a more significant reduction in pump power consumption can be achieved with the X-modification. For example, in the case of KCS-34, pumps power consumption is 125.53 kW at 70 bar (P_2) and 0.75 ammonia mass fraction (X_1), compared with 125.17 kW in the Y-modified cycle and 85.02 kW in the X-modified cycle.

Effect of turbine inlet pressure

At a fixed ammonia concentration on the working fluid and condensation pressure, the pump's power requirement gradually increases with the increasing turbine inlet pressure as the pump requires

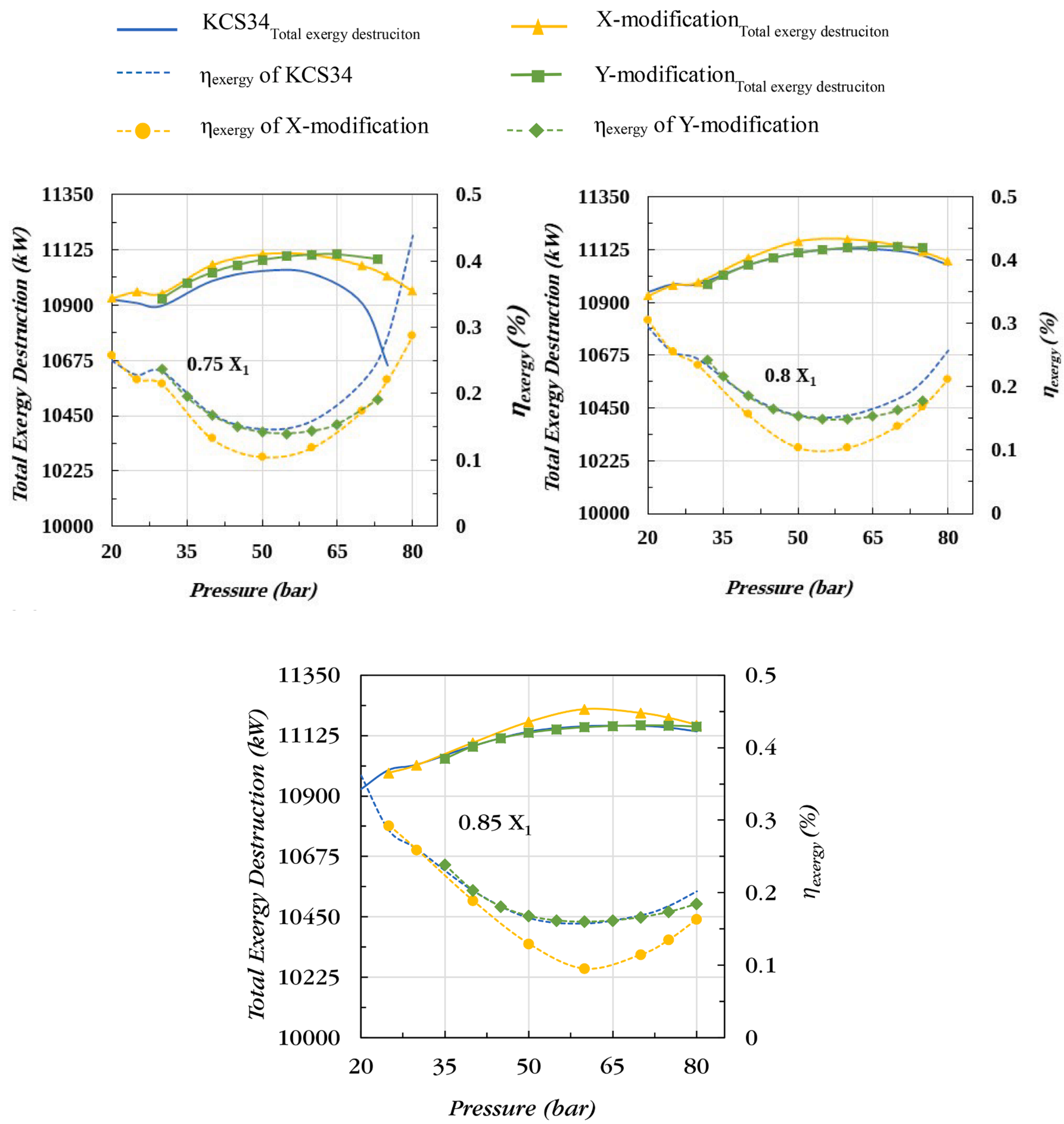

Fig. 8. Exergy destruction and Exergy efficiency with varying P_2.

additional power to raise the working fluid's pressure from the condensation pressure to higher turbine inlet pressure.

The correlation between turbine inlet pressure (P2) and pump power consumption is illustrated in Fig. 7. It can be seen from the figures that, in all the modifications of KCS-34, pump power consumption increases with the increase of P_2 at constant X_1. Thus, it is reasonable to conclude that the relationship between pressure P2 and pump power consumption is proportional.

Exergy destruction at various turbine inlet pressures

The exergy efficiency and exergy destruction curves for each of the three cases of the Kalina cycle have been represented in Fig. 8. At a fixed ammonia concentration with the increasing P_2, the exergy destruction rises up to a certain value; after reaching this peak point, exergy destruction decreases with increasing pressure. On the other hand, exergy efficiency is inversely proportional to exergy destruction, indicating that an increase in exergy efficiency decreases exergy destruction. However, not every component designed to operate in the cycle destroys the same amount of exergy. As an example, in Fig. 9, the exergy destruction for each component is represented at a working state of 60 bar and $0.85X_1$ and it can be observed that maximum exergy destruction can be observed at the condenser, whereas insignificant exergy destruction is seen in the separator.

Exergy destruction at various ammonia mass fraction

Fig. 10 represents the exergy destruction and exergy efficiency for all three cycles when the ammonia mass fraction varies at a constant P_2. The variation in exergy destruction with the changing ammonia concentration is minimal compared to the exergy destruction due to the varying P_2, indicating exergy's concise affectability to fluctuating ammonia concentration.

Energy recovered from the regenerators

Fig. 11 depicts the changes in energy recovery from the regenerator for all three cycles when the ammonia concentration in working fluid (X_1) has differed at a fixed P_2. At a fixed P_2, KCS-34 has the highest heat recovery capacity than the proposed modifications. Moreover, with

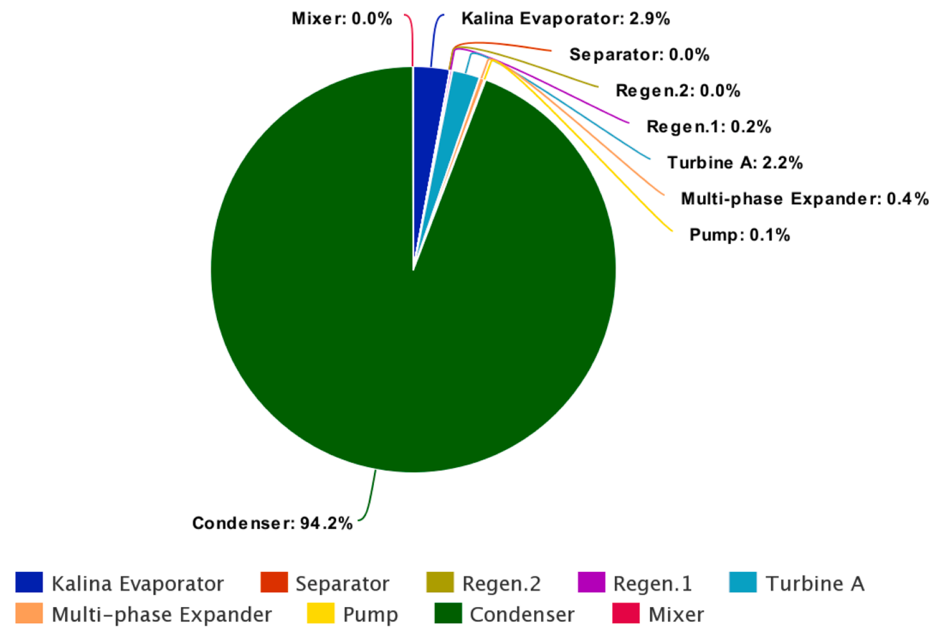

Fig. 9. Exergy destruction for individual components at 60 bar Turbine inlet pressure and 85% ammonia concentration on working fluid.

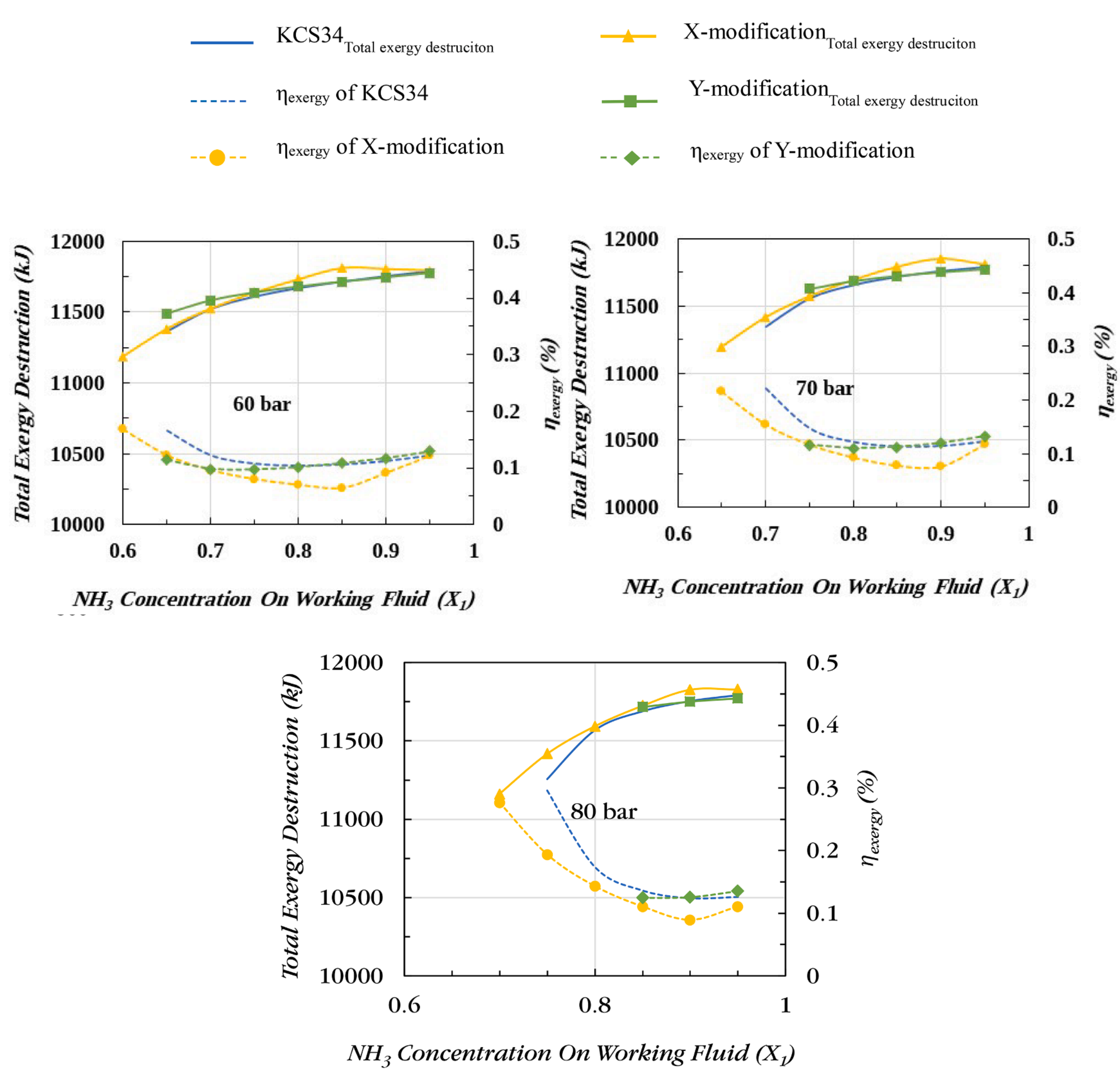

Fig. 10. Exergy destruction and Exergy efficiency with varying X_1

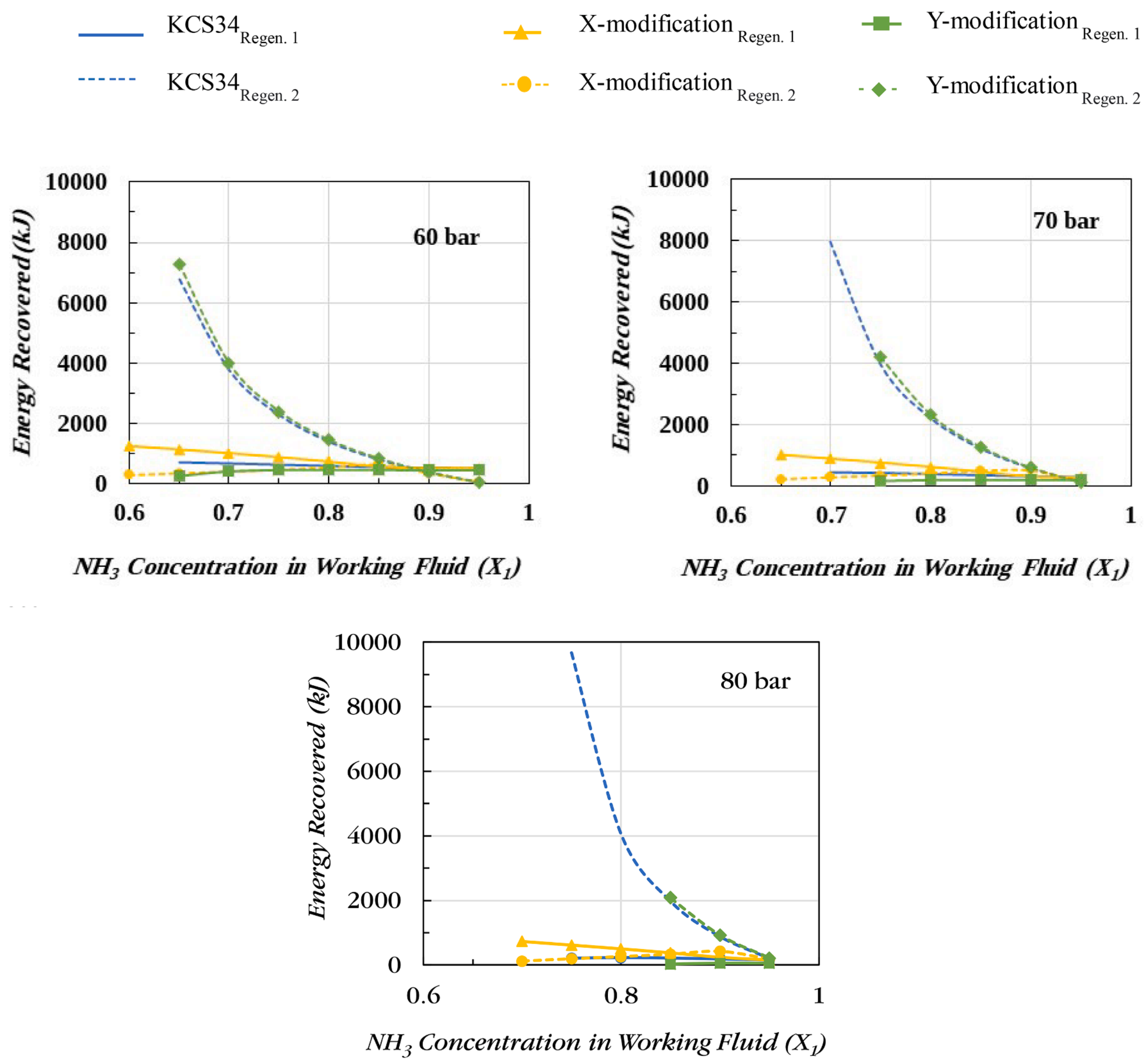

Fig. 11. Energy recovery from the regenerator with varying ammonia X_1.

increasing ammonia concentration in working fluid (X_1), the energy recovery from Regen. 1 and 2 get lower for the KCS-34 and X-modified cycle, whereas a negligible increase can be observed for the Y-modified cycle.

The variations in the amount of energy recovered from the regenerator for all three Kalina cycles under investigation are depicted in Fig. 12 when pressure P_2 is varied while maintaining a constant ammonia concentration in the working fluid (X_1). According to the different scenarios depicted in Fig. 12, with changing P2 at fixed ammonia concentration, energy recovery from Regen. 1 decrease with increasing P2 for all cases of KCS-34, whereas energy recovery from Regen. 2 increases with increasing P2. However, when compared to the case of fixed turbine inlet pressure, a similar trend of higher heat recovery for KCS-34 can be observed. Furthermore, the amount of heat recovered differs insignificantly between the three cycles.

Net power yield and efficiency analysis

Due to ammonia's lower specific heat capacity than water, the vapor generation rate at the Kalina evaporator goes up as the ammonia mass fraction in the working fluid increases. As a result, the rich ammonia-water mixture's mass flow rate increases across Turbine A, while the lean ammonia-water mixture's mass flow rate decreases across the multi-phase expander, leading to a rise in Turbine A's power output and decreased multi-phase expander power yield. This initially results in a higher net power output. However, when the ammonia mass fraction of the working fluid increases, the ammonia fraction in the turbine inlet increases, resulting in a decrease in the enthalpy variation across the turbine. The increase in rich ammonia-water mass flow across Turbine A is insufficient to compensate for the decline in enthalpy variation, resulting in a decrease in net power output following the peak point.

The relationship between turbine inlet pressure, thermal efficiency, and net power output of the Kalina cycles under consideration is illustrated in Fig. 13. At a lower turbine inlet pressure, it is observed that the KCS-34 produces more power and has a higher thermal efficiency than the other cycles. However, as the turbine inlet pressure increases, the Y-modified cycle outperforms different Kalina cycles investigated in this research in terms of net power output and thermal efficiency. For example, at 0.80 X_1, X-modified cycles' power output is higher when the turbine inlet pressure ranges between 30 bar and 70 bar; if the turbine inlet pressure surpasses 70 bar, higher power and efficiency can be derived from the Y-modified cycle. Thermal efficiency and power output do not increase with increasing power all the time in all the modifications; a pick can be observed. This pick demonstrates the maximum power output at a particular P_2.

When the turbine inlet pressure is increased, a significant decrease in enthalpy across the turbine is observed. The evaporation temperature rises, and the heat transfer rate reduces due to the constant difference in the pinch point temperature. However, in the evaporator, the ammonia-

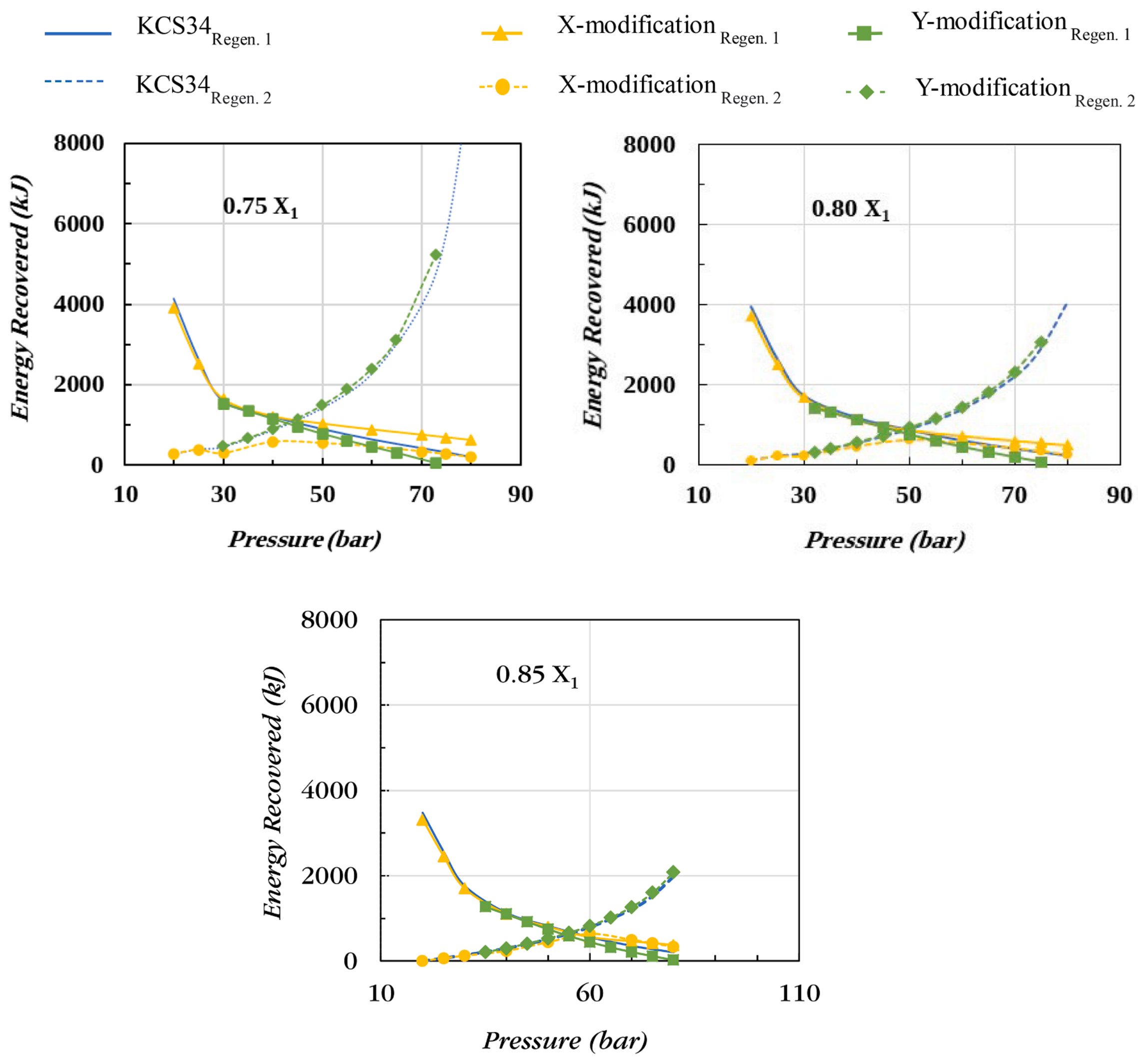

Fig. 12. Energy recovery from the regenerator with varying ammonia P_2.

water basic solution's heat absorption capacity per unit mass flow rate declines more significantly, resulting in a rise in the working fluid's mass flow rate. With the rising pressure in the separator, the rich ammonia-water mixture's flow rate decreases. The combined effect of the mass flow rate-rich ammonia-water mixture and the enthalpy drop results in an increase in net power output up to a certain point, after which it declines.

Fig. 14 describes the relationship between thermal efficiency and net power output with the varying ammonia concentration in the working substance. With the increasing ammonia mass fraction, the thermal efficiency and net power yield increase for the KCS-34 and Y-modified cycles. However, a peak can be noticed for the X-modified cycle, which indicates the optimum ammonia concentration in working fluid at a fixed P_2. For example, at 60 bar, the thermal efficiency and peak power yield can be observed at 0.86 X_1 for the X-modified cycle. The thermal efficiency and net power yield increase by 19.13% and 18.67%, respectively, for the Y-modified cycle, when the ammonia concentration is increased from 0.65 to 0.95.

In contrast, a 31.01% increase in power output and a 30.99% increase in thermal efficiency can be observed for KCS 34 when X_1 increased from 0.65 to 0.95. The thermal efficiency exhibits a comparative pattern similar to exergy efficiency; however, exergy efficiency is significantly higher compared to the thermal efficiency of the cycles. For instance, the Y-modified cycle's maximum exergy efficiency is 45% at 62 bar and 0.85 ammonia mass fraction; at similar operating conditions, the thermal efficiency is 17%.

In summary, from a thermodynamic perspective, the system's exergy and energy analysis indicate that the X-modified cycle is more desirable than the Y-modified cycle. It is concluded that it is more convenient to keep the ammonia concentration in the working fluid below its typical range for the proposed cycles. The variable temperature characteristics of the ammonia-water mixture can be used to illustrate this viewpoint. As presented in Fig. 15, the ammonia-water mixture's thermal drift varies with the ammonia's mass fraction. For mediocre ammonia concentration, the contrast within the bubble and dew point temperature resembles to be the optimum operating conditions for certain ammonia content.

Optimization results

The objective function for optimization was chosen to be exergy efficiency in this research. Due to the consistency of the heat source, inlet

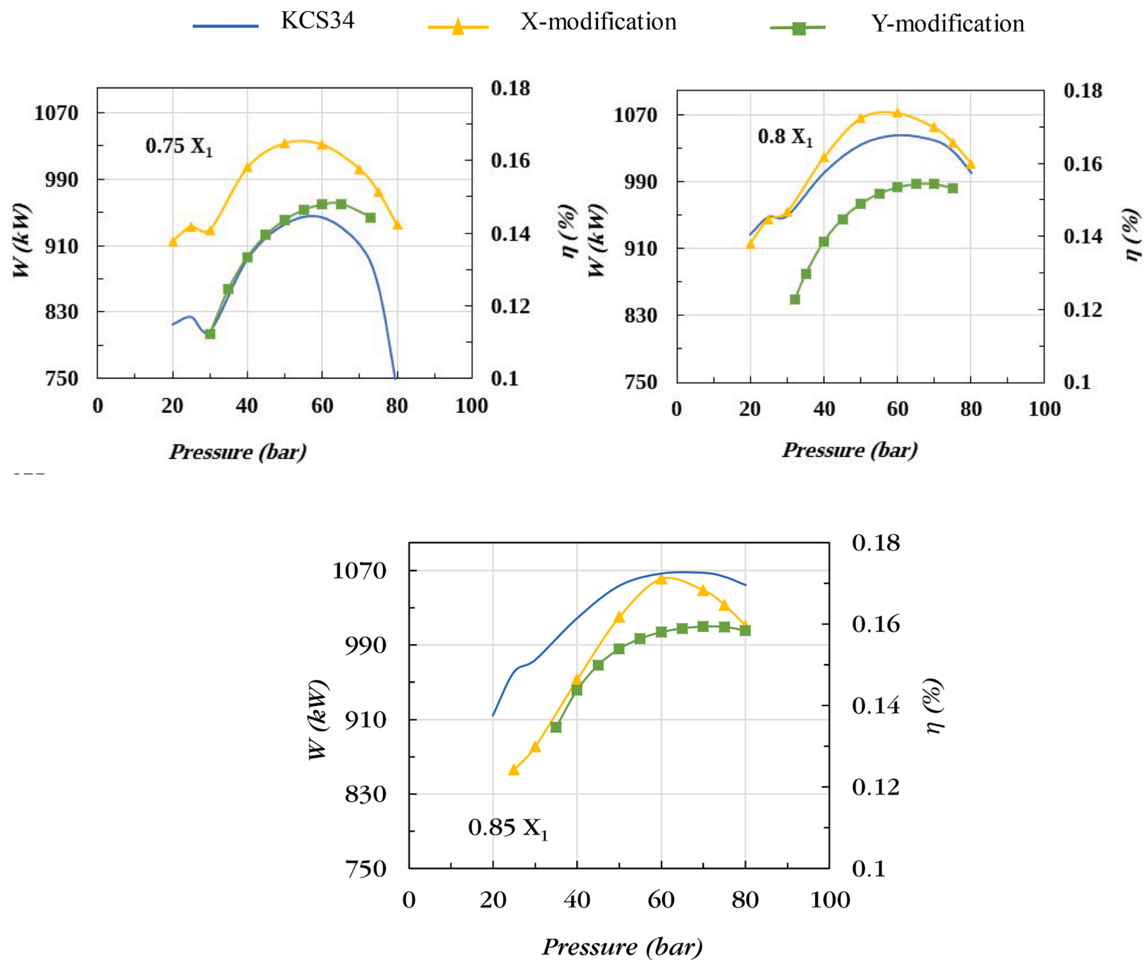

Fig. 13. Thermal efficiency and net power yield with varying turbine inlet pressure.

exergy remains constant for each optimization case; therefore, exergy efficiency is only dependent on net power output. In other words, by optimizing the exergy efficiency, the net power gets optimized. Three different ammonia concentration levels in the working fluid were optimized and all three cycles (including the two proposed cycles and base KCS-34 cycle) were considered. For the optimization purpose, the genetic algorithm, well known for its efficiency in finding the global optimum, was chosen. It can be observed that the optimum efficiencies of X-modification are generally higher than the other cases of the Kalina cycle under investigation. By analyzing the configuration of these cycles, the reason for this high value can be interpreted. For the Y-modified cycle, the multi-phase expander is positioned downstream of regen.2, conversely, for X-modification, it is positioned downstream of the separator. This results in a comparatively low energy flow at the inlet of Y-modification's multi-phase expander; therefore, power output declines and the efficiencies decrease subsequently. Thus, it can be concluded from the results that the X-modified cycle has superior performance in terms of efficiencies and power yield than other cases of KCS-34. For example, at 0.75 ammonia fraction, the power yield of X-modification is 4.57% and 1% higher than that of KCS 34 and Y-modification, respectively, which increases to 7.23% and 5.16% when ammonia mass fraction is 0.85.

The results are shown in Table 3, indicating different optimum points for different simulation cases.

Table 3 also points that as the ammonia concentration on working fluid increases, the optimum P_2 also increases, resulting in inconsistent evaporation temperature.Fig. 16

Conclusion

To maximize the thermodynamic performance of the low-enthalpy heat source driven KCS-34, the throttle valve is replaced with a multi-phase expander that extracts energy from the lean ammonia working fluid loop. Two different modifications have been analyzed when the heat source's temperature is 124 °C. Following that, the thermodynamic performance of all three cycles was optimized using a Genetic Algorithm, taking into account both the ammonia concentration in the working fluid and the turbine inlet pressure. From the derived results, the following conclusions can be drawn.

- Under a specific operating condition, X-modification's thermodynamic performance is better than the KCS-34 and Y-modification. For example, X-modification had a maximum 5.44% higher net power output than KCS-34 when 70 bar turbine inlet pressure (P_2) was specified; conversely, a maximum 7.83% higher net power output can be observed when compared with KCS-34 at an ammonia mass fraction of 0.85.
- When the thermodynamic performance of the proposed Kalina cycles was compared to that of the KCS-34 based Husavic

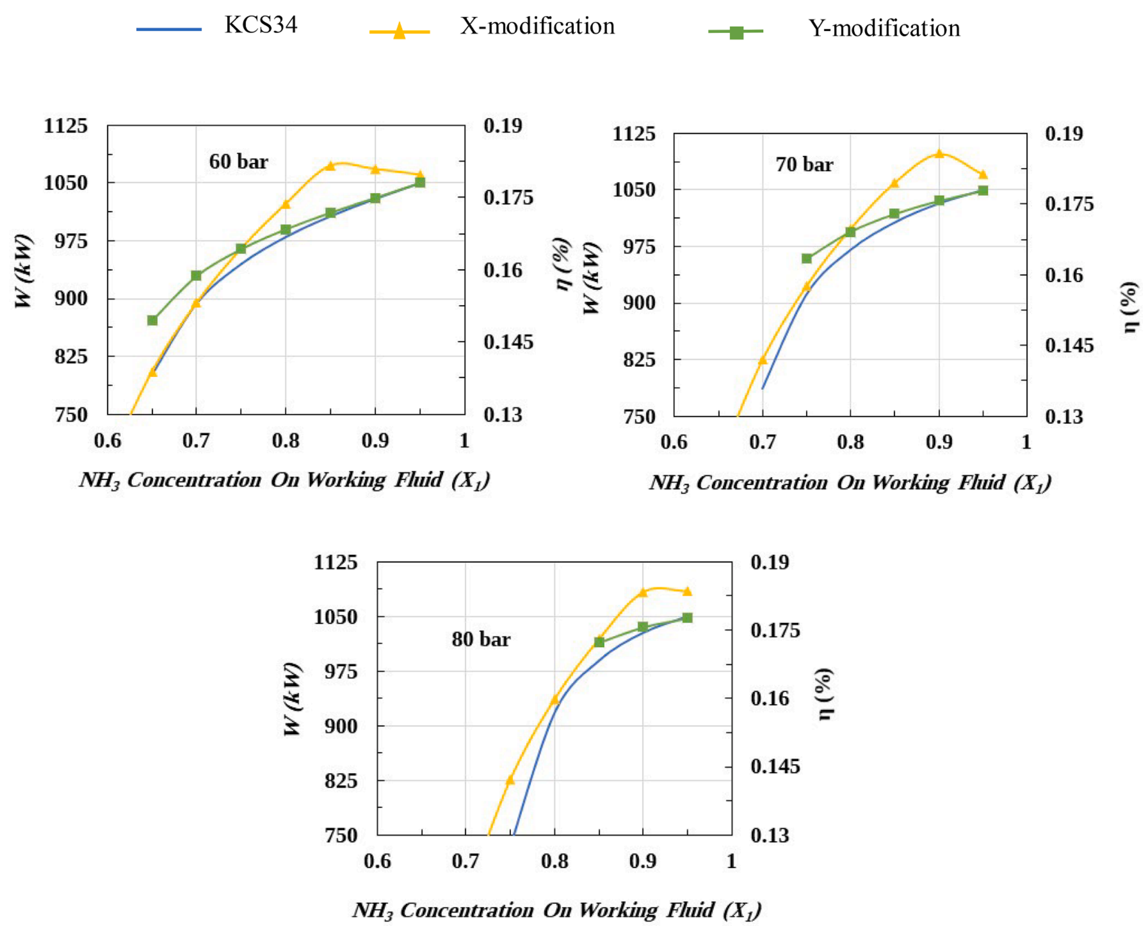

Fig. 14. Net power output and thermal efficiency with varying X_1

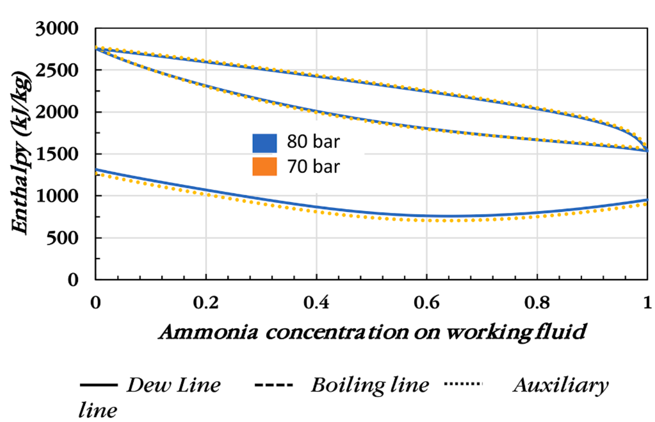

Fig. 15. Ammonia-water mixtures phase diagram

Power Plant [50] X-modified cycle generated 5.57% more power compared to KCS-34 based Husavic Power Plant.

- The only difference among the proposed cycle's layout is the multi-phase expander location relative to regen.2 and thermodynamic analysis reveals the dependency of the multi-phase expander's power output upon the regen.2.
- No significant thermodynamic advantage was observed for the Y-modified cycle when compared to the KCS-34. Additionally, when the Y-modifications are implemented on KCS-34, the ammonia concentration range becomes more constrained, which arduous the possibility for an off-design utilization of Y-modified cycle.
- The maximum exergy destruction was observed in the condenser, making the condenser a crucial component of the Kalina cycle system and optimization procedure.

However, the Kalina cycles proposed in this research can be further

Table 3
Under similar operating condition optimization of cycles under investigation.

X_1	Power output (kW)			P_2			η			Destruction (kJ)			Exergy efficiency		
	KCS 34	X-cycle	Y-cycle	KCS 34	X-cycle	Y-cycle	KCS 34	X-cycle	Y-cycle	KCS 34	X-cycle	Y-cycle	KCS 34	X-cycle	Y-cycle
0.75	921	965	956	57	55	62	0.16	0.16	0.16	10,410	10,288	10,396	0.4	0.41	0.41
0.8	955	1015	983	60	58	66	0.17	0.17	0.17	10,416	10,273	10,420	0.42	0.43	0.42
0.85	983	1060	1005	63	62	71	0.17	0.18	0.17	10,429	10,262	10,449	0.43	0.45	0.43

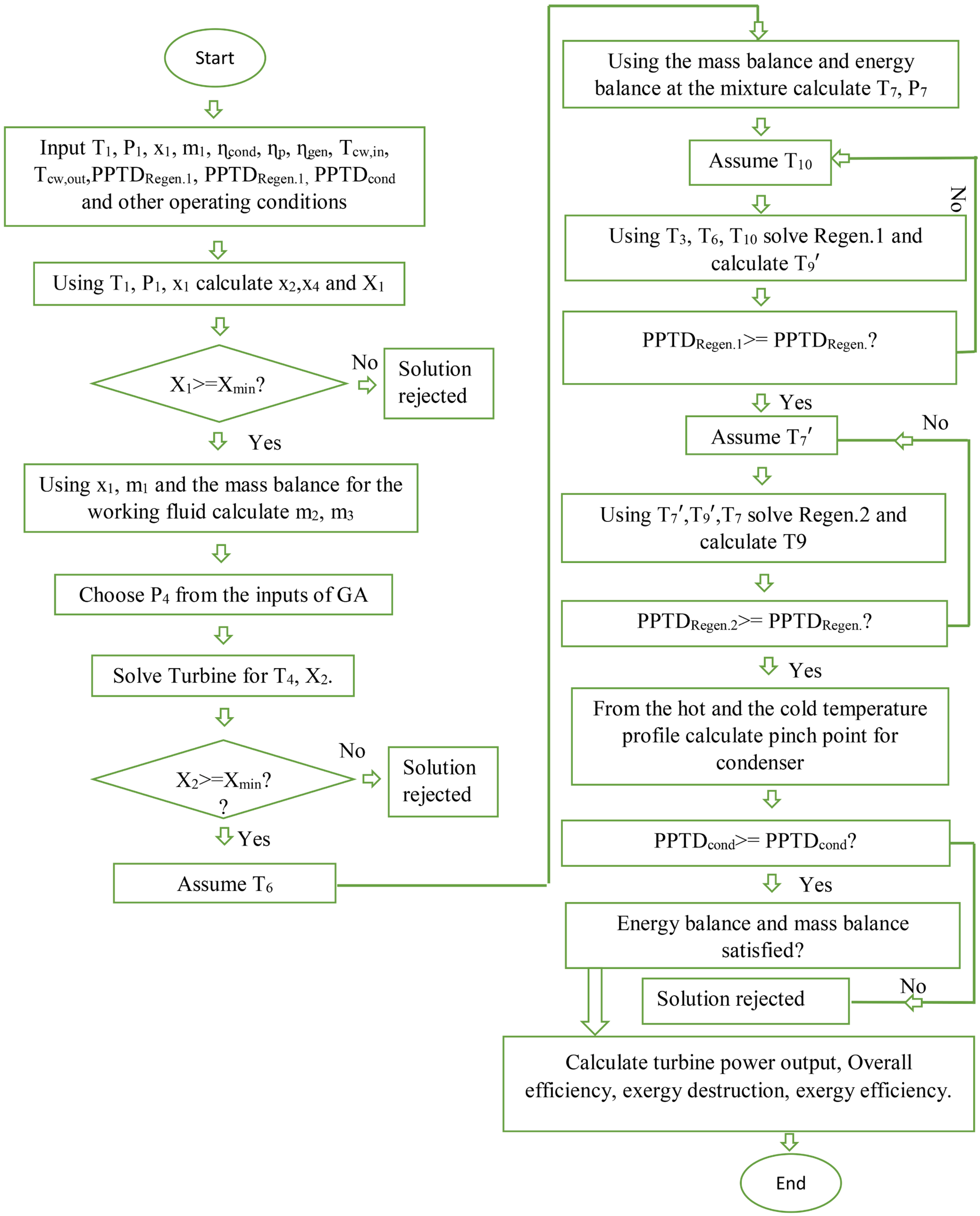

Fig. 16. Detailed optimization algorithm for the KCS-34

investigated to determine their suitability for other applications, such as in the waste heat recovery system or as a bottoming cycle. The mathematical model presented in this study is capable of being used successfully for these purposes.

CRediT authorship contribution statement

Mohammad Masrur Hossain: Conceptualization, Methodology, Formal analysis, Writing – original draft. **Niyaz Afnan Ahmed:** Conceptualization, Methodology, Formal analysis, Writing – review & editing. **Md Abid Shahriyar:** Methodology, Writing – review & editing. **M. Monjurul Ehsan:** Formal analysis, Writing – review & editing. **Fahid Riaz:** Writing – review & editing. **Sayedus Salehin:** Writing – review & editing. **Chaudhary Awais Salman:** Supervision, Writing – review & editing.

Declaration of Competing Interest

The authors declare that they have no known competing financial interests or personal relationships that could have appeared to influence the work reported in this paper.

References

[1] Riaz F, Lee PS, Chou SK. Thermal modelling and optimization of low-grade waste heat driven ejector refrigeration system incorporating a direct ejector model. Appl Therm Eng 2020;167:114710. https://doi.org/10.1016/j.applthermaleng.2019.114710.
[2] Riaz F, Lee PS, Chou SK, Ranjan R, Tay CS, Soe T. Analysis of low-grade waste heat driven systems for cooling and power for tropical climate. Energy Procedia 2017;143:389–95. https://doi.org/10.1016/j.egypro.2017.12.701.
[3] Riaz F, Farooq M, Imran M, Lee PS, Chou SK, "Energy Analysis of a New Combined Cooling and Power System for Low-Temperature Heat Utilization," Jun. 2020, doi: 10.1115/ES2020-1658.
[4] Riaz F, et al. Design and energy analysis of a solar desiccant evaporative cooling system with built-in daily energy storage. Energies 2021;14(9):2429. https://doi.org/10.3390/en14092429.
[5] Nafey AS, Sharaf MA. Combined solar organic Rankine cycle with reverse osmosis desalination process: energy, exergy, and cost evaluations. Renew. Energy 2010;35(11):2571–80. https://doi.org/10.1016/j.renene.2010.03.034.
[6] Madhawa Hettiarachchi HD, Golubovic M, Worek WM, Ikegami Y. Optimum design criteria for an Organic Rankine cycle using low-temperature geothermal heat sources. Energy 2007;32(9):1698–706. https://doi.org/10.1016/j.energy.2007.01.005.
[7] Guo J, Xu M, Cheng L. Thermodynamic analysis of waste heat power generation system. Energy 2010;35(7):2824–35. https://doi.org/10.1016/j.energy.2010.03.012.
[8] Riaz F, Tan KH, Farooq M, Imran M, Lee PS. Energy analysis of a novel ejector-compressor cooling cycle driven by electricity and heat (waste heat or solar energy). Sustainability 2020;12(19):8178. https://doi.org/10.3390/su12198178.
[9] Gao H, Liu C, He C, Xu X, Wu S, Li Y. Performance analysis and working fluid selection of a supercritical organic rankine cycle for low grade waste heat recovery. Energies 2012;5(9):3233–47. https://doi.org/10.3390/en5093233.
[10] He C, et al. The optimal evaporation temperature and working fluids for subcritical organic Rankine cycle. Energy 2012;38(1):136–43. https://doi.org/10.1016/j.energy.2011.12.022.
[11] He J, Liu C, Xu X, Li Y, Wu S, Xu J. Performance research on modified KCS (Kalina cycle system) 11 without throttle valve. Energy 2014;64:389–97. https://doi.org/10.1016/j.energy.2013.10.059.
[12] Mirolli MD, "The kalina cycle for cement kiln waste heat recovery power plants," In *Conference Record Cement Industry Technical Conference, 2005.*, 2005, vol. 2005, pp. 330–336, doi: 10.1109/CITCON.2005.1516374.
[13] Shukla PR, Biswas D, Nag T, Yajnik A, Heller T, Victor DG. Impact of power sector reforms on technology, efficiency and emissions: case study of Andhra Pradesh, India. Power 2004;(March).
[14] Iyer C, Bajpai MP. Review of risks associated with renovation modernization of thermal power plants in India. Pressacademia 2017;5(1):169–75. https://doi.org/10.17261/Pressacademia.2017.586.
[15] Chikkatur AP, Sagar AD, Abhyankar N, Sreekumar N. Tariff-based incentives for improving coal-power-plant efficiencies in India. Energy Policy 2007;35(7):3744–58. https://doi.org/10.1016/j.enpol.2007.01.006.
[16] P. R. Shukla, D. Biswas, T. Nag, A. Yajnik, T. Heller, and D. G. Victor, "Impact of Power Sector Reforms on Technology , Efficiency and Emissions : Case Study of Andhra Pradesh , India," *Power*, no. March, 2004, Accessed: Jan. 03, 2021. [Online]. Available: https://pesd.fsi.stanford.edu/publications/impact_of_power_sector_reforms_on_technology_efficiency_and_emissions_case_study_of_gujarat_india.
[17] Zhang X, He M, Zhang Y. A review of research on the Kalina cycle. Renew Sustain Energy Rev 2012;16(7):5309–18. https://doi.org/10.1016/j.rser.2012.05.040.
[18] Kalina AI. Combined-cycle system with novel bottoming cycle. J Eng Gas Turbines Power 1984;106(4):737–42. https://doi.org/10.1115/1.3239632.
[19] Nasruddin, Usvika R, Rifaldi M, Noor A. Energy and exergy analysis of kalina cycle system (KCS) 34 with mass fraction ammonia-water mixture variation. J Mech Sci Technol 2009;23(7):1871–6. https://doi.org/10.1007/s12206-009-0617-8.
[20] Nag PK, Gupta AVSSKS, "Exergy analysis of the Kalina cycle," *Appl. Therm. Eng.*, 18 (6), pp. 427–439, 1998, doi: 10.1016/S1359-4311(97)00047-1.
[21] Mlcak H, Mirolli M, Hjartarson H, Húsavíkur O, Ralph M. Notes from the North: A Report on the Debut Year of the 2 MW Kalina Cycle® Geothermal Power Plant in Húsavík, Iceland. Trans - Geothermal Resour Council 2002:715–8.
[22] Madhawa Hettiarachchi HD, Golubovic M, Worek WM, Ikegami Y. The Performance of the Kalina Cycle System 11(KCS-11) With Low-Temperature Heat Sources. J Energy Resour Technol 2007;129(3):243–7. https://doi.org/10.1115/1.2748815.
[23] Goswami DY, Xu F. Analysis of a new thermodynamic cycle for combined power and cooling using low and mid temperature solar collectors. J Sol Energy Eng 1999;121(2):91–7. https://doi.org/10.1115/1.2888152.
[24] Xu F, Yogi Goswami D, Bhagwat SS. A combined power/cooling cycle. Energy 2000;25(3):233–46. https://doi.org/10.1016/S0360-5442(99)00071-7.
[25] Vidal A, Best R, Rivero R, Cervantes J. Analysis of a combined power and refrigeration cycle by the exergy method. Energy 2006;31(15):3401–14. https://doi.org/10.1016/j.energy.2006.03.001.
[26] Liu M, Zhang N. Proposal and analysis of a novel ammonia-water cycle for power and refrigeration cogeneration. Energy 2007;32(6):961–70. https://doi.org/10.1016/j.energy.2006.09.012.
[27] Sun F, Ikegami Y, Jia B. A study on Kalina solar system with an auxiliary superheater. Renew Energy 2012;41:210–9. https://doi.org/10.1016/j.renene.2011.10.026.
[28] Xie N, Liu Z, Luo Z, Ren J, Deng C, Yang S. Multi-objective optimization and life cycle assessment of an integrated system combining LiBr/H2O absorption chiller and Kalina cycle. Energy Convers Manag 2020;225(July):113448. https://doi.org/10.1016/j.enconman.2020.113448.
[29] Soltani M, Nabat MH, Razmi AR, Dusseault MB, Nathwani J. A comparative study between ORC and Kalina based waste heat recovery cycles applied to a green compressed air energy storage (CAES) system. Energy Convers Manag 2020;222(July):113203. https://doi.org/10.1016/j.enconman.2020.113203.
[30] Rostamzadeh H, Ebadollahi M, Ghaebi H, Shokri A. Comparative study of two novel micro-CCHP systems based on organic Rankine cycle and Kalina cycle. Energy Convers. Manag 2019;183(July 2018):210–29. https://doi.org/10.1016/j.enconman.2019.01.003.
[31] Parikhani T, Jannatkhah J, Shokri A, Ghaebi H. Thermodynamic analysis and optimization of a novel power generation system based on modified Kalina and GT-MHR cycles. Energy Convers Manag 2019;196(December 2018):418–29. https://doi.org/10.1016/j.enconman.2019.06.018.
[32] Köse Ö, Koç Y, Yağlı H. Energy, exergy, economy and environmental (4E) analysis and optimization of single, dual and triple configurations of the power systems: Rankine Cycle/Kalina Cycle, driven by a gas turbine. Energy Convers Manag 2021;227(August 2020):113604. https://doi.org/10.1016/j.enconman.2020.113604.
[33] Gogoi TK, Hazarika P. Comparative assessment of four novel solar based triple effect absorption refrigeration systems integrated with organic Rankine and Kalina cycles. Energy Convers Manag 2020;226(July):113561. https://doi.org/10.1016/j.enconman.2020.113561.
[34] Malik MZ, Musharavati F, Khanmohammadi S, Pakseresht AH, Khanmohammadi S, Nguyen DD. Design and comparative exergy and exergo-economic analyses of a novel integrated Kalina cycle improved with fuel cell and thermoelectric module. Energy Convers Manag 2020;220(June):113081. https://doi.org/10.1016/j.enconman.2020.113081.
[35] Zhou C, Zhuang Y, Zhang L, Liu L, Du J, Shen S. A novel pinch-based method for process integration and optimization of Kalina cycle. Energy Convers Manag 2020;209(2):112630. https://doi.org/10.1016/j.enconman.2020.112630.
[36] Mohammadkhani F, Yari M, Ranjbar F, "A zero-dimensional model for simulation of a Diesel engine and exergoeconomic analysis of waste heat recovery from its exhaust and coolant employing a high-temperature Kalina cycle," *Energy Convers. Manag.*, 198(July), p. 111782, 2019, doi: 10.1016/j.enconman.2019.111782.
[37] Abdolalipouradl M, Khalilarya S, Jafarmadar S, "Exergoeconomic analysis of a novel integrated transcritical CO2 and Kalina 11 cycles from Sabalan geothermal power plant," *Energy Convers. Manag.*, 195(August 2018), pp. 420–435, Sep. 2019, doi: 10.1016/j.enconman.2019.05.027.
[38] Rafat E, Babaelahi M, "Recovering waste heat of a solar hybrid power plant using a Kalina cycle and desalination unit: A sustainability (emergo-economic and emergo-environmental) approach," *Energy Convers. Manag.*, 224(August), p. 113394, Nov. 2020, doi: 10.1016/j.enconman.2020.113394.
[39] Zhang S, Chen Y, Wu J, Zhu Z, Fang F, "Thermodynamic analysis on a Kalina cycle based power and chilling refrigeration cogeneration cycle," *Appl. Therm. Eng.*, 161 (July), p. 114077, Oct. 2019, doi: 10.1016/j.applthermaleng.2019.114077.
[40] Dhahad HA, Hussen HM, Nguyen PT, Ghaebi H, Ashraf MA, "Thermodynamic and thermoeconomic analysis of innovative integration of Kalina and absorption refrigeration cycles for simultaneously cooling and power generation," *Energy Convers. Manag.*, 203(June 2019), p. 112241, 2020, doi: 10.1016/j.enconman.2019.112241.
[41] Smith IK, Stosic N, "Prospects for energy conversion efficiency improvements by the use of twin screw two-phase expanders," in *2nd International Heat Power Cycles Conference, Paris, France.*, 2001, vol. 35263.
[42] Brasz JJ, Smith IK, Stosic N, "Development of a Twin Screw Expressor as a Throttle Valve Replacement for Water-Cooled Chillers," *Int. Compress. Eng. Conf.*, Jan. 2000,

Accessed: Nov. 29, 2020. [Online]. Available: https://docs.lib.purdue.edu/icec/1488.
[43] Tchanche BF, Lambrinos G, Frangoudakis A, Papadakis G. Exergy analysis of micro-organic Rankine power cycles for a small scale solar driven reverse osmosis desalination system. Appl Energy 2010;87(4):1295–306. https://doi.org/10.1016/j.apenergy.2009.07.011.
[44] Papadopoulos AI, Stijepovic M, Linke P. On the systematic design and selection of optimal working fluids for Organic Rankine Cycles. Appl Therm Eng 2010;30(6–7):760–9. https://doi.org/10.1016/j.applthermaleng.2009.12.006.
[45] Uehara H, Ikegami Y. Optimization of a closed-cycle OTEC system. J Sol Energy Eng 1990;112(4):247–56. https://doi.org/10.1115/1.2929931.
[46] Bliem C, Zangrando F, Hassani V, "Value analysis of advanced heat rejection systems for geothermal power plants," in *IECEC 96. Proceedings of the 31st Intersociety Energy Conversion Engineering Conference*, 1996, vol. 3, pp. 1616–1621, doi: 10.1109/IECEC.1996.553342.
[47] Bombarda P, Invernizzi CM, Pietra C. Heat recovery from Diesel engines: A thermodynamic comparison between Kalina and ORC cycles. Appl Therm Eng 2010;30(2–3):212–9. https://doi.org/10.1016/j.applthermaleng.2009.08.006.
[48] El-Sayed YM, Tribus M, "Theoretical comparison of the rankine and kalina cycles.," in *American Society of Mechanical Engineers, Advanced Energy Systems Division (Publication) AES*, 1985, vol. 1, pp. 97–102, Accessed: Dec. 29, 2020. [Online]. Available: https://jglobal.jst.go.jp/en/detail?JGLOBAL_ID=200902040063886118.
[49] Wall G. Exergy study of the kalina cycle. Am Soc Mech Eng 1989.
[50] Ogriseck S. Integration of Kalina cycle in a combined heat and power plant, a case study. Appl Therm Eng 2009;29(14–15):2843–8. https://doi.org/10.1016/j.applthermaleng.2009.02.006.
[51] Yari M, Mehr AS, Zare V, Mahmoudi SMS, Rosen MA. Exergoeconomic comparison of TLC (trilateral Rankine cycle), ORC (organic Rankine cycle) and Kalina cycle using a low grade heat source. Energy 2015;83:712–22. https://doi.org/10.1016/j.energy.2015.02.080.
[52] Dejfors C, Thorin E, Svedberg G. Ammonia–water power cycles for direct-fired cogeneration applications. Energy Convers Manag 1998;39(16–18):1675–81. https://doi.org/10.1016/S0196-8904(98)00087-9.